International Journal of Environmental Science and Technology
https://doi.org/10.1007/s13762-023-05265-1

ORIGINAL PAPER

Crop height estimation of sorghum from high resolution multispectral images using the structure from motion (SfM) algorithm

E. Tunca[1] · E. S. Köksal[2] · S. Çetin Taner[2] · H. Akay[3]

Received: 19 September 2022 / Revised: 12 May 2023 / Accepted: 8 October 2023

Abstract

Crop height (CH) is the key indicators of crop growth, biomass and yield. However, obtaining CH information with manual measurement is inefficient for larger areas. High-resolution unmanned air vehicle (UAV) images offer a new alternative to traditional CH measurements. In this study, we compared three approaches to estimate sorghum CH using high-resolution multispectral images based on structure from motion (SfM) algorithm and spectral vegetation indices. In the first approach, CH was estimated based on the difference between the Digital Surface Model (DSM) map and Digital Terrain Model (DTM) map generated from UAV images captured immediately after the sowing. In the second approach, DTM was generated from DSM. In the last approach, CH was estimated using the spectral vegetation indices. High-resolution multispectral images were obtained at 40 m above ground level elevation. Ground control points were laid around the study area, and these point positions were determined using a GPS device. DSM and DTM images were generated from 3D point cloud data and the SfM algorithm. Results showed that the SfM technique could estimate sorghum CH accurately using DSM, DTM and GCPs ($R^2 = 0.97$, RMSE = 8.77 cm, MAPE = 5.98%). Also, a high correlation was observed between estimated and measured sorghum CH using DTM maps generated from DSM maps (R^2, RMSE, MAPE were 0.94, 12.2 cm, 6.66%). Moreover, GNDVI was the best vegetation index to estimate sorghum CH ($R^2 = 0.81$, RMSE = 24.6 cm, MAPE = 12.56%). Overall, this study demonstrates the UAV potential for CH estimates and reducing the cost of obtaining CH information.

Editorial responsibility: Samareh Mirkia.

✉ E. Tunca
emretunca@duzce.edu.tr

[1] Biosystem Engineering, Agriculture Faculty, Düzce University, Düzce, Turkey

[2] Department of Agricultural Structures and Irrigation, Agriculture Faculty, Ondokuz Mayıs University, Samsun, Turkey

[3] Department of Field Crops, Agriculture Faculty, Ondokuz Mayıs University, Samsun, Turkey

Published online: 27 October 2023

Graphical abstract

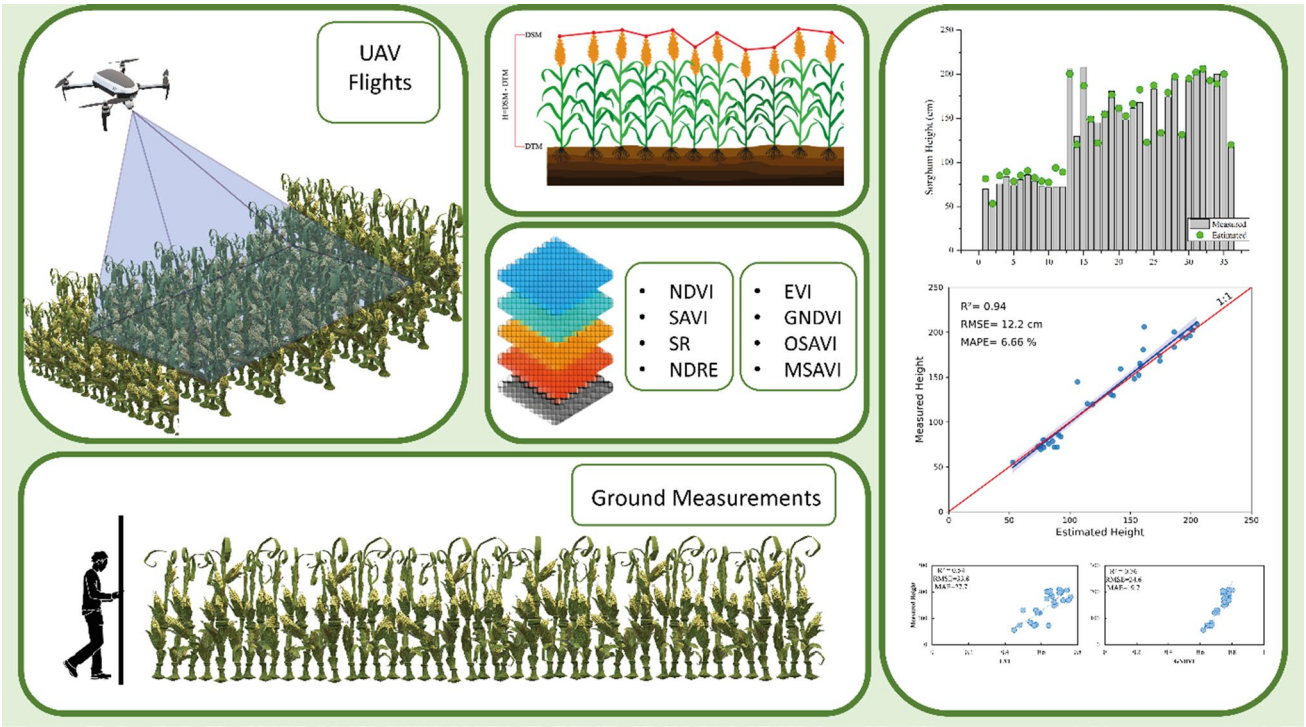

Keywords Unmanned air vehicle · Sorghum · Crop height estimation · Structure from motion · GNDVI · Digital surface model

Introduction

Crop height (CH) is defined as the vertical distance between the land surface and the upper boundary of the main photosynthetic tissues (Volpato et al. 2021). Rapid and accurate CH information is a vital component of precision agriculture (Luo et al. 2021) and plays a crucial role in yield estimation (Malambo et al. 2018), carbohydrate storage capacity (Xie and Yang 2020), sensitivity of lodging (Hassan et al. 2019) and crop classification (Aasen et al. 2015). Traditionally, crop development has been evaluated by measuring CH, and this data is often gathered in field measurements with a simple metric ruler (Luo et al. 2021). However, this method is laborious, time-consuming, prone to measurement error, and only applicable to small-scale fields (Mielcarek et al. 2018; Yuan et al. 2018). Therefore, existing CH measurement methods cannot obtain timely and accurate CH information in large-scale locations, particularly throughout the various crop development stages.

Satellite and aerial remote sensing can capture repeated multi-temporal vegetation information in agricultural fields during the crop growing periods and have also been used for estimation of leaf area index (Gao et al. 2020), canopy cover (Lu et al. 2021), biomass (Li et al. 2020), evapotranspiration (Aboutalebi et al. 2020) and CH (Lang et al. 2019). However, CH estimation from optical remote sensing is seldom studied. Although optical remote sensing platforms such as satellite images provide valuable spectral data, they can obtain only two dimensions of remotely sensed data, which cannot directly incorporate information about vegetation's vertical structure (Schulze-Brüninghoff et al. 2019). In addition, optical remote sensing is limited by the saturation

Fig. 1 The geographical location of the study area within Samsun, Turkey

problem in the high LAI field areas (Tunca et al. 2018). Therefore, the estimation of CH by using remotely sensed optical data has great limitations and needs a new technique to precisely estimate CH. Several researchers have reported that Light Detection and Ranging (LiDAR) techniques offer a new option to obtain CH information based on aerial and terrestrial remote sensing platforms. For example, Anthony et al. (2014) conclude that corn height can be estimated within 5 cm by LiDAR data. In a study conducted by Holman et al. (2016), it was demonstrated that wheat height could be estimated using the LiDAR sensor with an R^2 of 0.97. Harkel et al.

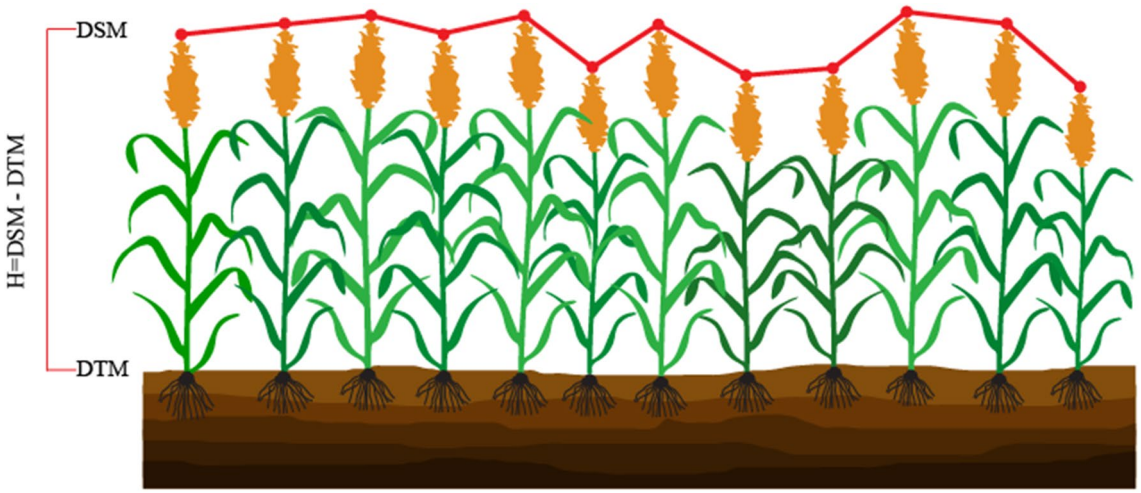

Fig. 2 Showing the calculation of estimated sorghum crop height by using the digital surface map and digital terrain map

Table 1 Equations used to calculate vegetation indices to estimate sorghum crop height

Vegetation Index	Formula	Source
Normalized difference vegetation index (NDVI)	$\frac{(NIR-RED)}{(NIR+RED)}$	(Rouse et al. 1974)
Soil adjusted vegetation index (SAVI)	$(1+L)\times\frac{(NIR-RED)}{(L+NIR+RED)}$	(Huete 1988)
Band ratio (RATIO)	$\frac{NIR}{RED}$	(Tucker 1979)
Normalized Difference Red Edge Index (NDRE)	$\frac{(NIR-REDEDGE)}{(NIR+REDEDGE)}$	(Barnes et al. 2000)
Enhanced Vegetation Index (EVI)	$G\times\frac{(NIR-RED)}{NIR+(C1\times RED-C2\times BLUE)+L}$	(Liu and Huete 1995)
Green Normalized Difference Vegetation Index (GNDVI)	$\frac{(NIR-GREEN)}{(NIR+GREEN)}$	(Gitelson et al. 1996)
Optimized Soil Adjusted Vegetation Index (OSAVI)	$(1+Y)\times\frac{(NIR-RED)}{(NIR+RED+Y)}$	(Rondeaux et al. 1996)
Modified soil adjusted vegetation index (MSAVI)	$\frac{2\times NIR+1-\sqrt{(2\times NIR+1)^2-8\times(NIR-RED)}}{2}$	(Qi et al. 1994)

NIR, RED, GREEN, REDEDGE and BLUE refer to the specific reflectance bands of the Micasense Altum multispectral camera. L is a soil adjustment factor in the SAVI equation. G = 2.5, C1 = 6, C2 = 7.5, L = 1 and Y = 0.16 in the EVI equation

(2020) investigated the potential use of data acquired from LiDAR to estimate different crop heights (potato, sugar beet, and winter wheat). Results showed that crop heights could be estimated precisely (< 12 cm) by LiDAR data. Although LiDAR data can generate higher laser point density, which can improve the estimation of CH, it can increase the data collection cost, especially for large-scale fields (Jakubowski et al. 2013). Furthermore, LiDAR data volumes can be very large, which could be a problem for storage and processing (Yuan et al. 2018).

With the advancements in sensor technologies and the area of computer vision, techniques such as structure from motion (SfM) are starting to be used with high-resolution unmanned aerial vehicle (UAV) images to estimate CH because of their low cost and high spatial and temporal resolution (Xie et al. 2021). In SfM, high-resolution overlapped images are used to construct 3D canopy architecture. This approach enables UAV data to generate point clouds of comparable quality to LiDAR, which is critical for accurately investigating canopy structures (Xie et al. 2021). Several attempts have been made to use high-resolution UAV images to estimate CH in wheat (Holman et al. 2016), sorghum (Watanabe et al. 2017), barley (Bendig et al. 2014), and maize (Malambo et al. 2018).

To date, only a few studies have investigated the factors affecting CH estimation based on UAV images. Therefore, this study compares and evaluates different CH estimation methods with ground CH measurements. Also, the impact of different point cloud densities and UAV flight heights on CH estimation was evaluated.

The rest of the paper is organized as follows. Sect. "Materials and methods" provides the details of the methods used in this study Sect. "Results and discussion" contains results and discussion of this study and finally Sect. "Conclusion" concludes the paper.

Materials and methods

Study area and field experiments

The study (Fig. 1) was conducted at Black Sea Agricultural Research Institute, Samsun, Turkey (41°36′ N, 35°55′ E and

Table 2 The results of the statistical analysis of measured and estimated sorghum crop height

	R^2	RMSE (cm)	MAPE (%)
59 DAS (13 July 2020)	0.64	9.76	10.92
82 DAS (05 August 2020)	0.85	10.84	5.22
111 DAS (03 September 2020)	0.98	4.24	1.79
All Dates	0.97	8.77	5.98

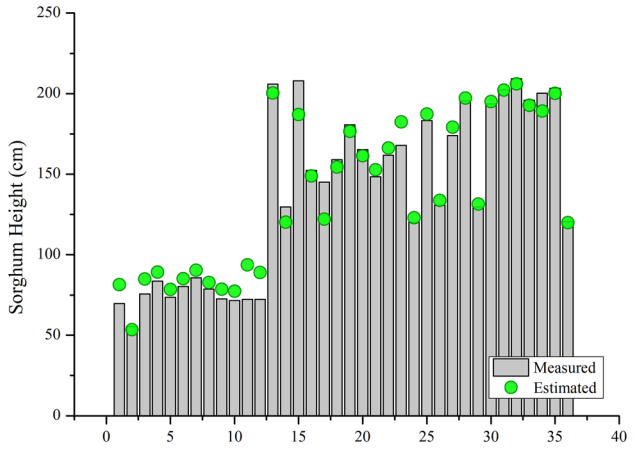

Fig. 3 Comparison of estimated and measured sorghum height using GCP and DSM data

15 m above sea level) in a 0.1 ha research field with 5 cm within rows and 70 cm between rows of sorghum. The study area has a sub-humid climate, with rainfall and reference evapotranspiration (ET_o) of 126.6 and 672.6 mm, respectively, during the sorghum growing periods in 2020. Soils in the study area are silty-loam. In this study, four different irrigation treatments were applied to the plots. Irrigation levels were as follows: (i) Full irrigation (S1), (ii) 70% of S1 (S2), (iii) 40% of S1 (S3), and (iv) rainfed, which was not irrigated after the starting of the irrigation treatments. Experiment plots were planted as randomized block designs with three replications. The plot's size is 9.6 m^2 (eight rows and 8 m long). Sowing of sorghum seeds was carried out on May 15th,2020 at a density of approximately 35 seed m^{-2}.

Unmanned air vehicle data acquisition

High-resolution multispectral UAV images were acquired with DJI Matrice 600 (DJI, Shenzhen, China) on July 13th (59 Days after sowing, DAS), August 5th (82 DAS) and September 3rd (111 DAS) in 2020 based on sorghum development stages at an elevation of 40 m above ground level. In addition, on September 3rd, study area images were obtained from 40 and 120 m above ground level to assess the effect of UAV flight height on sorghum CH estimation. Study area images were captured with Micasense Altum (MicaSense, Seattle, USA) camera. This camera has five multispectral and one thermal sensor. Radiometric calibration of the multispectral bands was performed with a calibration panel and irradiance sensor that monitors solar energy. Geometric correction of the images was performed using the four ground control points (GCP). The positions of these points were measured using a global positioning system device (Geo7x, Trimble GeoExplorer, USA). All UAV flights were conducted in cloudless conditions, and images were acquired at solar noon. Flight planning had 90/90 frontal and side overlaps, respectively, and a double grid mission plan was applied.

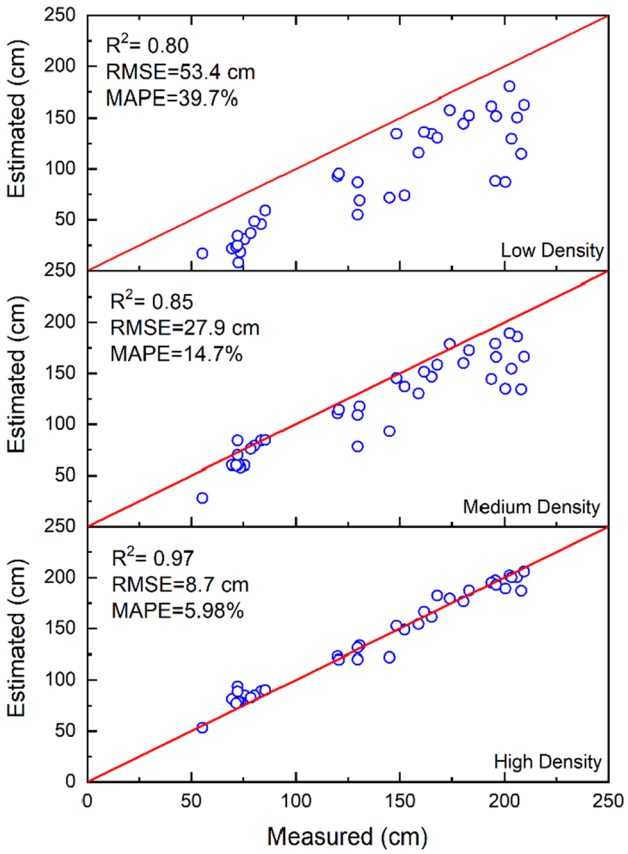

Fig. 4 Scatter plots of ground measured sorghum crop height values versus estimated based on SfM: (top) low density, (middle) medium density, (bottom) high density

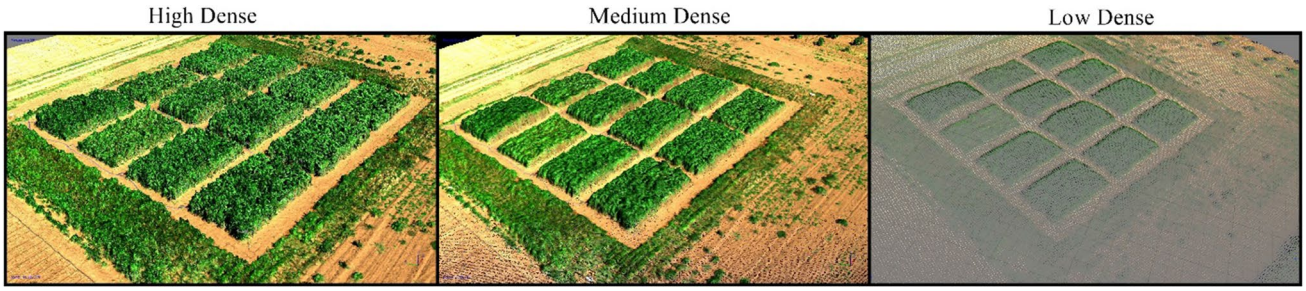

Fig. 5 Sorghum canopy construction model based on different dense point clouds: (left) high dense, (middle) medium dense, (right) low dense

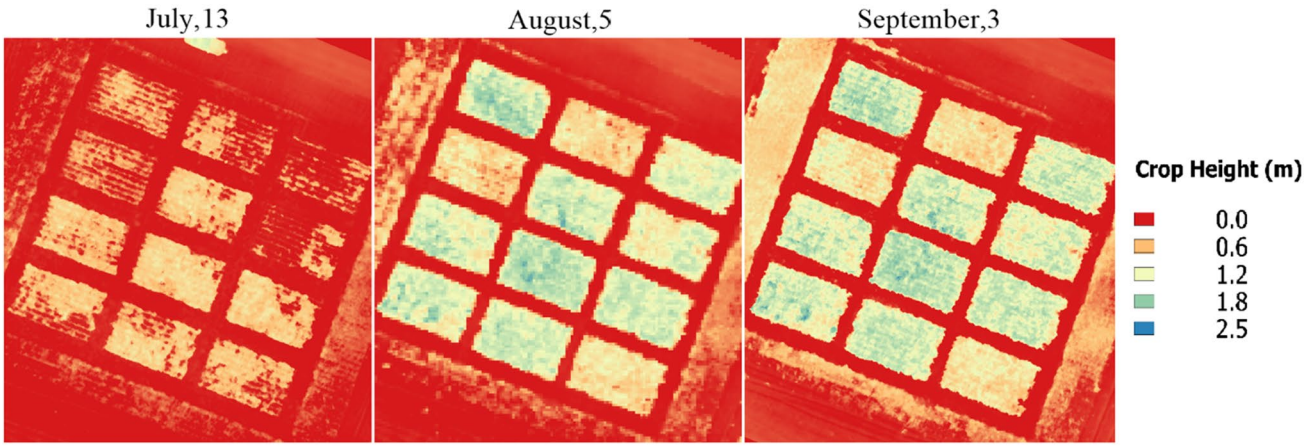

Fig. 6 Resulting sorghum height maps using only DTM images

Ground CH measurements

In situ, sorghum CH was measured in the per plots as ground truth data to compare with the estimated sorghum CH values using high-resolution UAV images. For this, four representative plants from each plot were measured with a simple ruler from the ground to the top leaf of the sorghum crop during the vegetative period or from ground to tassel in the reproductive period (Malambo et al. 2018). CH was calculated for each plot by averaging all the measurements. Ground CH measurements were conducted on July 10th (56 DAS), August 5th (82 DAS), and September 3rd (111 DAS).

Sorghum CH estimation by using the SfM algorithm

In this study, estimated sorghum CH values were calculated using the difference between the digital surface model

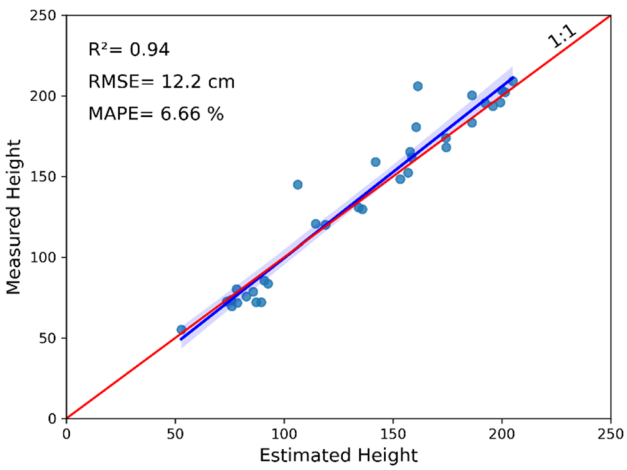

Fig. 7 Comparison between measured and estimated sorghum height without DSM

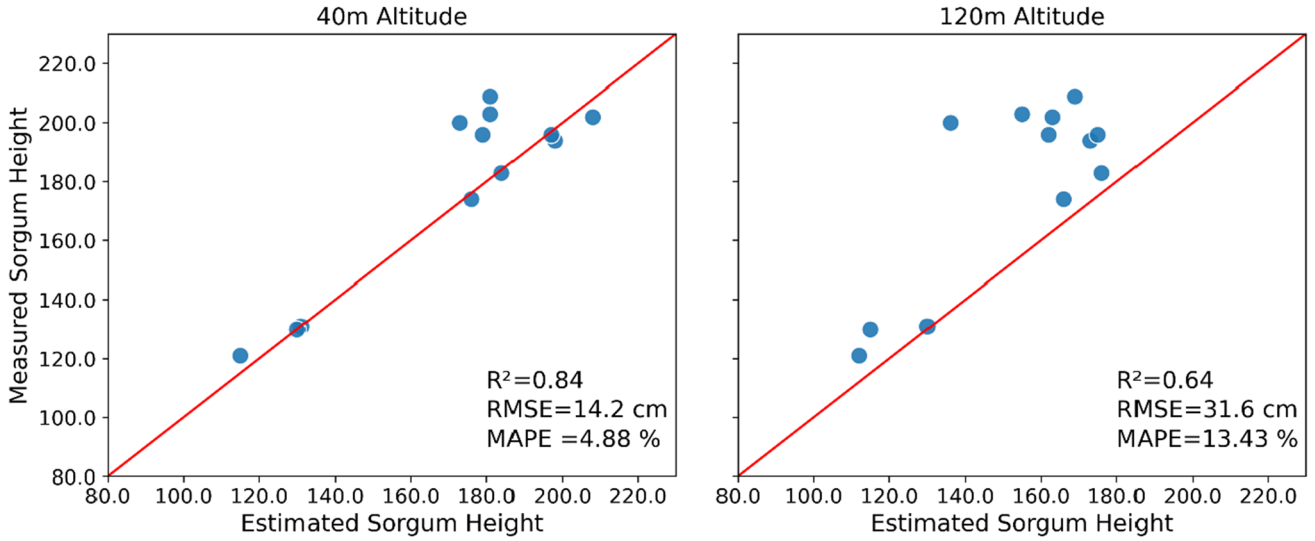

Fig. 8 Comparison of estimated sorghum height at different flight altitude versus ground measured

(DSM) and digital terrain model (DTM) derived from UAV images taken immediately after the sowing (Fig. 2). DSM and DTM images were generated using the Agisoft Metashape (Agisoft LLC, Petersburg, Russia) software. This software utilizes SfM algorithms to the images to obtain DTM or DSM. SfM algorithm matches the feature points of the objects from multiple overlapped images to generate a 3D model (Bendig et al. 2013; Stanton et al. 2017). Dense point cloud and DSM were generated based on the determined camera position. In this study, estimation of sorghum CH was also performed using DSM images solely. For this, non-vegetative areas were classified as ground, and these points were interpolated to generate a DTM image. Finally, sorghum CH estimation maps were calculated by subtracting DSM from DTM. Details can be found in Xie et al. (2021).

Table 3 Effects of different flight altitude (40 m and 120 m) on estimation of sorghum height

	Sum of squares	df	Mean square	F	p-Significant
Between groups	1998.92	1	1998.92	2.82	0.1069
Within groups	15,564.42	22	707.47		
Total	17,563.34	23			

Sorghum CH estimation using the vegetation indices

Several researchers estimated CH from remotely sensed data (Payero et al. 2004; Xie et al. 2021). This study evaluated eight commonly used spectral vegetation indices to estimate sorghum CH (Table 1). According to Georgios et al. (2010), an exponential relationship between the spectral vegetation indices and CH was the best. Due to this, we tested exponential regression models to estimate sorghum CH using the spectral vegetation indices.

Statistical analysis

The coefficient of determination (R^2), root mean square error (RMSE), and mean absolute percentage error (MAPE) were used to evaluate the accuracy and robustness of the sorghum CH estimation models. R^2, RMSE, and MAPE have commonly used evaluation metrics in research because they provide important insights into the model's accuracy and allow for a thorough evaluation of its performance (Küçüktopcu 2023). While R^2 values show the level of the model fitting, RMSE and MAPE values indicate the accuracy of the models. R^2, RMSE, and MAPE were calculated using Eqs. 1,2 and 3.

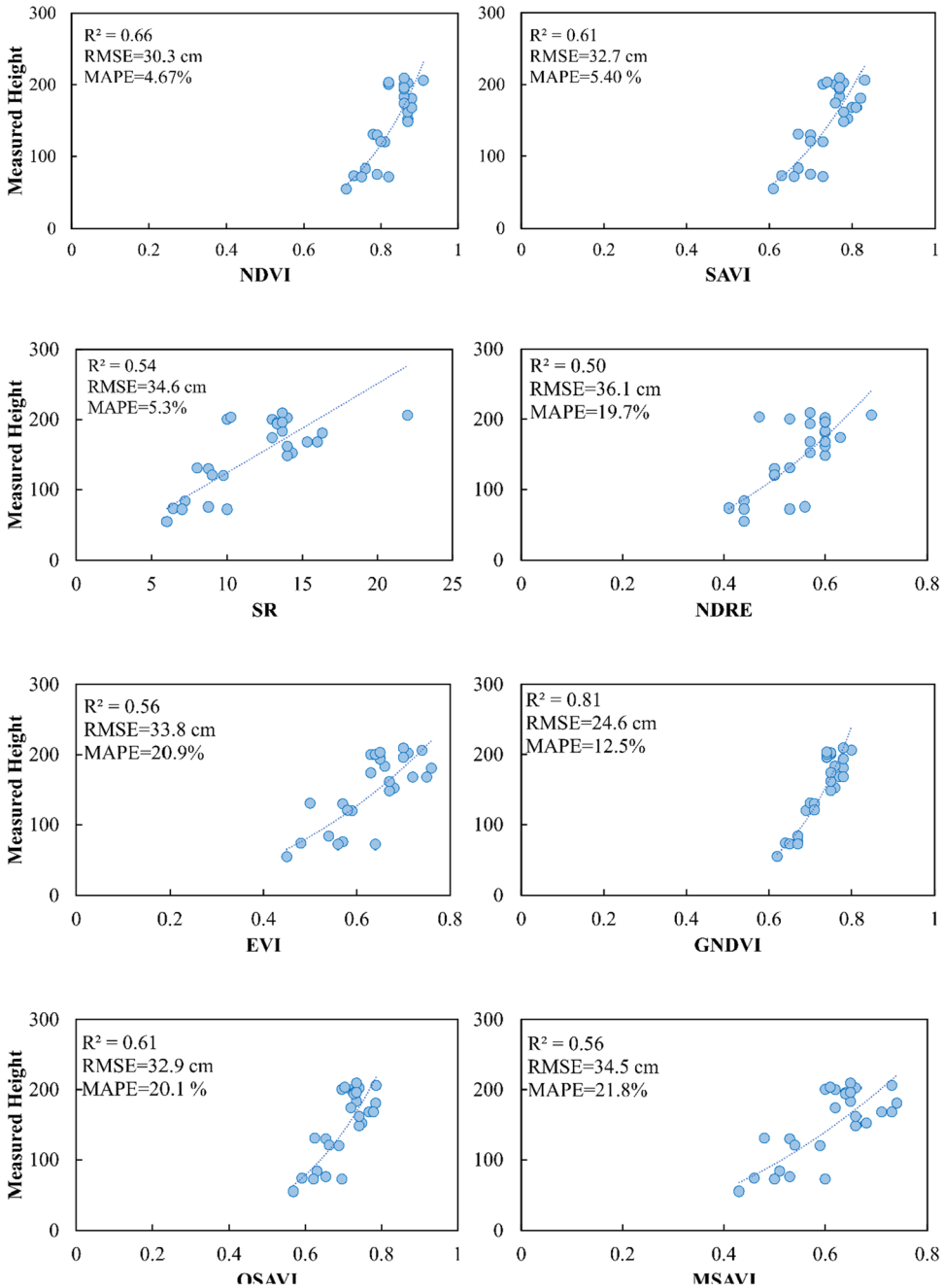

Fig. 9 Statistical results of sorghum heights using spectral vegetation indices calculated from high-resolution multispectral images

$$R^2 = 1 - \frac{\sum_{i=1}^{n}\left(M_i - E_i\right)^2}{\sum_{i=1}^{n}\left(M_i - \overline{M_i}\right)^2} \quad (1)$$

$$RMSE = \sqrt{\frac{\sum_{i=1}^{n}\left(M_i - E_i\right)^2}{n}} \quad (2)$$

$$MAPE = \frac{1}{n}\sum_{1}^{n}\frac{|M_i - E_i|}{M_i} \quad (3)$$

where, M_i *and* E_i are denote measured and estimated CH, respectively, n indicates the number of observations.

Results and discussion

Comparison of estimated and measured sorghum CH

To reveal each plot's homogeneity level, the standard deviation of the SfM-based estimated sorghum CH values was determined for each date. In all cases, standard deviation values were lower than 25%, indicating that experiment plots are relatively homogenous (van Iersel et al. 2018). Based on these results, field measured values were compared with each plot's average estimated CH value.

Statistical analysis was performed between estimated sorghum CH values created by subtracting DTM from DSM and field-measured sorghum CH values. There was a statistically significant positive correlation ($p < 0.001$) between SfM-derived and field-measured sorghum CH. Table 2 summarizes the accuracy level of this relationship. 111 DAS achieved the highest R^2 (0.98) with RMSE and MAPE of 4.24 cm and 1.79%, respectively followed by 82 DAS ($R^2 = 0.85$, RMSE = 10.84 cm, MAPE = 5.22%). The lowest R^2 values were obtained at 59 DAS ($R^2 = 0.64$, RMSE = 9.76 cm, MAPE = 10.92%). These results are consistent with those obtained by Xie et al. (2021), who reported that R^2 of measured versus estimated CH values using DTM and GCPs ranged from 0.81 to 0.93. Also, this result seems to be consistent with Blanquart et al. (2020)'s results which showed that crop height was estimated with an RMSE of 8.2 cm, and when removed the systematic error, this value decreased to 5.8 cm.

Figure 3 presents the estimated sorghum CH values versus measured values. While estimated sorghum CH values range from 53.38 to 206.05 cm (mean = 139.28 cm), most measured sorghum CH values range from 55.33 to 203.3 cm and in some dates, up to 209.33 cm. As Fig. 3 shows, estimated sorghum CH values are generally higher than the measured values, which are likely attributed to ground control errors or moving of the plant due to wind during the image capturing. Several reports have shown that windy weather conditions during the UAV flight mission could cause some blurring of the images, thereby it makes challenging to match the points between the images (Chang et al. 2017; Han et al. 2018; van Iersel et al. 2018). While the most consistent results were obtained from 111 DAS, the inconsistent results were obtained in 59 DAS. This low correlation in 59 DAS could be explained by the number of days separating UAV flight camping (59 DAS) and field measurement (56 DAS). For that example, sorghum crops were in the developing period and were rapidly growing during this time, so three days difference could cause a substantial difference. Generally, the success rate of the sorghum CH estimation increased from 59 to 111 DAS. Malambo et al. (2018) stated that the precision of SfM algorithms could vary during the crop growing period. Also, the results of this study are in accordance with Grenzdörffer (2014) report, which concluded that the SfM algorithm performs better in dense canopy areas than in sparse ones.

Impact of the point cloud density and using DSM on CH estimation

The impact of different point cloud densities (high, medium, and low) on sorghum CH estimation is shown in Fig. 4. Also, Fig. 5 shows the sorghum canopy construction model generated using three types of dense point clouds. The results revealed that sorghum CH estimation precision varied with the point cloud's density. While RMSE and MAPE values were lower with higher point density ($R^2 = 0.97$, RMSE = 8.77 cm, MAPE = 5.98%), larger errors were calculated with lower point density ($R^2 = 0.80$, RMSE = 53.42 cm, MAPE = 39.73%). Generally, sorghum CHs were underestimated with the decrease in the point density. This caused to increase in the RMSE and MAPE values. However, R^2 values were not affected significantly, which still shows the sorghum CH trends. This indicates that, the SfM technique requires high-resolution DSM and DTM images generated from denser point clouds to obtain accurate sorghum CH. These results agree with Harkel et al. (2020) results which showed that overall errors of lower point density were higher than that of the high point density. Also, Luo et al. (2021) indicated that maize and soybean

CH estimation precision dropped rapidly with the decreasing point density.

In this study, sorghum CH was also estimated by using only DTM images. For this, non-vegetated areas were classified as ground, and these points were interpolated to generate an artificial DSM image. Finally, sorghum CH estimation maps were generated by subtracting DSM from DTM. The resulting sorghum CH maps are shown in Fig. 6. Estimated sorghum CH values were extracted from these images and compared with ground measurements, and results were given in Fig. 7. Estimated sorghum CH values across the three dates showed consistent trends with field measured values, and R^2 was calculated as 0.94 (RMSE = 12.2 cm and MAPE = 6.66%). The study result indicates that this approach can achieve comparable results, and this technique is quite suitable for estimating sorghum CH. In addition, GCPs could not be necessary, which needs labor. However, this technique could be useless when the canopy cover is dense since it is hard to find bare soil points. In our case, the area between the plots was bare soil, and the terrain was almost flat. However, when the surface is not flat or fully covered by the crop, DSM image must be acquired before the sowing/immediately after sowing, or DSM values must be extracted before the full vegetation cover.

Overall, the RMSE and MAPE statistics indicate that using DSM (high density) with GCPs produces a low error level of sorghum CH. However, it needs to lay out GCPs in the area and acquisition the position of these points. These processes are time-consuming and need more labor (Yue et al. 2017). Furthermore, measuring the position of the GCPs requires devices such as high precession GPS instruments. Therefore, using GCPs to estimate CH is challenging to implement and needs additional costs (Xie et al. 2021).

Impact of the UAV flight height on CH estimation

In this study, the influence of the different UAV flight heights (40 m and 120 m) on the sorghum CH estimation was evaluated. The scatterplot of estimated sorghum CH values for different UAV flight altitudes against measured sorghum CH values is shown in Fig. 8. A one-way ANOVA test was carried out to show differences between estimated sorghum CH values at different flight heights (Table 3). Results showed no significant differences between the flight altitude for estimating sorghum CH, indicating that UAV flight altitude did not influence sorghum CH estimation statistically. Estimated sorghum CH values were generally consistent with measured sorghum CH values. R^2 values for 40 m and 120 m UAV flight height estimation were obtained as 0.84 and 0.64 ($p < 0.001$). A higher RMSE value (31.6 cm) was obtained for 120 m altitude, and the lower RMSE value (14.2 cm) was determined for 40 m altitude. Although some differences exist between estimated and measured sorghum CH values at different UAV flight heights, the results indicate that the differences are not statistically significant. Therefore, sorghum CH could be successfully estimated at an elevation of 120 m above ground level. Also, users can prefer 120 m to cover a larger area and minimize UAV data collection costs.

CH estimation based on spectral indices

Sorghum CH estimation as a function of spectral vegetation indices is shown in Fig. 9, which includes all measured sorghum CH values during the growing periods. It shows that sorghum CH values increased exponentially as the vegetation indices increased, which indicates spectral vegetation indices are saturated to show the differences in sorghum CH. These results are consistent with Payero et al. (2004), who concluded that CH estimation based on spectral vegetation indices is insensitive to CH's changes due to saturation of the vegetation indices. As seen in Fig. 4, GNDVI obtained the best sorghum CH estimation results, with an R^2 value of 0.81, and RMSE and MAPE values are 24.6 cm and 12.5%, respectively. The lowest R^2 value (0.48) was obtained using the NDRE (RMSE = 36.1 cm, MAPE = 19.7%).

Conclusion

The information on CH is vital for agricultural research to monitor the crops during the growing periods. Manual CH data collection can result in measurement errors and requires labor to obtain accurate CH values. CH estimation using high-resolution UAV images can be used to estimate the CH of the entire study area. In this study, sorghum CH values were estimated from UAV images using the SfM technique and compared with ground measurements. The results of this study indicated that using the SfM technique establishes a greater degree of accuracy in estimating sorghum CH. The RMSE and MAPE between estimated and measured CH were 8.77 cm and 5.98%, respectively, using the high-density point cloud. These results demonstrated that the SfM technique is capable of estimating sorghum CH and can be used for crop phenotyping during the crop growing period. Moreover, calculated CH values can be used to estimate yield or biomass before the harvest. Also, this study evaluated the role of point density and DSM in estimating sorghum CH. Results showed that the SfM technique based on high point density could precisely estimate sorghum CH. Another significant practical implication result is that sorghum CH can be estimated accurately without DSM data. In this approach, R^2,

RMSE, and MAPE were calculated as 0.94, 12.2 cm, and 6.66%, respectively. However, when the surface is covered by vegetation or the ground is not flat, this approach can introduce some errors. Moreover, sorghum CH can be estimated using spectral vegetation indices. The highest accuracy was achieved with the GNDVI ($R^2 = 0.76$, RMSE = 24.6 cm, and MAPE = 12.5%), but using the spectral vegetation indices to estimate CH hardly affected the saturation of the vegetation index. This method can be used as an alternative to estimate sorghum CH when the vegetation indices are in a sensitive period of CH change. In the future, further studies will need to be carried out to estimate CH for different plants and climate zones. Also, further research is needed to understand better the impact of the UAV sensors and flight altitude to estimate CH.

Acknowledgements This research was supported by Scientific and Technological Research Council of Turkey (Grant Numbers: 118O831)

Declarations

Conflict of interest The authors declare that they have no conflicts of interest.

References

Aasen H, Burkart A, Bolten A, Bareth G (2015) Generating 3D hyperspectral information with lightweight UAV snapshot cameras for vegetation monitoring: from camera calibration to quality assurance. ISPRS J Photogramm Remote Sens 108:245–259

Aboutalebi M, Torres-Rua AF, McKee M, Kustas WP, Nieto H, Alsina MM, White A, Prueger JH, McKee L, Alfieri J (2020) Incorporation of unmanned aerial vehicle (UAV) point cloud products into remote sensing evapotranspiration models. Remote Sens 12:50

Anthony D, Elbaum S, Lorenz A, Detweiler C (2014) On crop height estimation with UAVs. In: 2014 IEEE/RSJ international conference on intelligent robots and systems (pp. 4805–4812): IEEE

Barnes E, Clarke T, Richards S, Colaizzi P, Haberland J, Kostrzewski M, Waller P, Choi C, Riley E, Thompson T (2000) Coincident detection of crop water stress, nitrogen status and canopy density using ground based multispectral data. In: Proceedings of the fifth international conference on precision agriculture, Bloomington, MN, USA

Bendig J, Bolten A, Bennertz S, Broscheit J, Eichfuss S, Bareth G (2014) Estimating biomass of barley using crop surface models (CSMs) derived from UAV-based RGB imaging. Remote Sens 6:10395–10412

Bendig J, Bolten A, Bareth G (2013) 4 UAV-based imaging for multi-temporal, very high resolution crop surface models to monitor crop growth variability. Unmanned aerial vehicles (UAVs) for multi-temporal crop surface modelling, 44

Blanquart J-E, Sirignano E, Lenaerts B, Saeys W (2020) Online crop height and density estimation in grain fields using LiDAR. Biosys Eng 198:1–14

Chang A, Jung J, Maeda MM, Landivar J (2017) Crop height monitoring with digital imagery from Unmanned Aerial System (UAS). Comput Electron Agric 141:232–237

Gao R, Nassar A, Aboutalebi M, Torres-Rua AF, Prueger JH, McKee L, Alfieri JG, Hipps L, Nieto H, White WA (2020) Grapevine Leaf Area Index Estimation with Machine Learning and Unmanned Aerial Vehicle Information. In: AGU Fall Meeting Abstracts (pp. H008-0012)

Georgios P, Diofantos HG, Kyriacos T, Leonidas T (2010) Spectral vegetation indices from field spectroscopy intended for evapotranspiration purposes for spring potatoes in Cyprus. In: Remote sensing for agriculture, ecosystems, and hydrology XII (p. 782410): International Society for Optics and Photonics

Gitelson AA, Kaufman YJ, Merzlyak MN (1996) Use of a green channel in remote sensing of global vegetation from EOS-MODIS. Remote Sens Environ 58:289–298

Grenzdörffer G (2014) Crop height determination with UAS point clouds. Int Archiv Photogramm Remote Sens Spatial Inf Sci 40:135

Han X, Thomasson JA, Bagnall GC, Pugh N, Horne DW, Rooney WL, Jung J, Chang A, Malambo L, Popescu SC (2018) Measurement and calibration of plant-height from fixed-wing UAV images. Sensors 18:4092

Harkel J, Bartholomeus H, Kooistra L (2020) Biomass and crop height estimation of different crops using UAV-based LiDAR. Remote Sensing 12:17

Hassan MA, Yang M, Fu L, Rasheed A, Zheng B, Xia X, Xiao Y, He Z (2019) Accuracy assessment of plant height using an unmanned aerial vehicle for quantitative genomic analysis in bread wheat. Plant Methods 15:1–12

Holman FH, Riche AB, Michalski A, Castle M, Wooster MJ, Hawkesford MJ (2016) High throughput field phenotyping of wheat plant height and growth rate in field plot trials using UAV based remote sensing. Remote Sens 8:1031

Huete AR (1988) A soil-adjusted vegetation index (SAVI). Remote Sens Environ 25:295–309

Jakubowski MK, Guo Q, Kelly M (2013) Tradeoffs between lidar pulse density and forest measurement accuracy. Remote Sens Environ 130:245–253

Küçüktopcu E (2023) Comparative analysis of data-driven techniques to predict heating and cooling energy requirements of poultry buildings. Buildings 13:142

Lang N, Schindler K, Wegner JD (2019) Country-wide high-resolution vegetation height mapping with Sentinel-2. Remote Sens Environ 233:111347

Li B, Xu X, Zhang L, Han J, Bian C, Li G, Liu J, Jin L (2020) Above-ground biomass estimation and yield prediction in potato by using UAV-based RGB and hyperspectral imaging. ISPRS J Photogramm Remote Sens 162:161–172

Liu HQ, Huete A (1995) A feedback based modification of the NDVI to minimize canopy background and atmospheric noise. IEEE Trans Geosci Remote Sens 33:457–465

Lu J, Cheng D, Geng C, Zhang Z, Xiang Y, Hu T (2021) Combining plant height, canopy coverage and vegetation index from UAV-based RGB images to estimate leaf nitrogen concentration of summer maize. Biosys Eng 202:42–54

Luo S, Liu W, Zhang Y, Wang C, Xi X, Nie S, Ma D, Lin Y, Zhou G (2021) Maize and soybean heights estimation from unmanned aerial vehicle (UAV) LiDAR data. Comput Electron Agric 182:106005

Malambo L, Popescu SC, Murray SC, Putman E, Pugh NA, Horne DW, Richardson G, Sheridan R, Rooney WL, Avant R (2018) Multitemporal field-based plant height estimation using 3D point clouds generated from small unmanned aerial systems high-resolution imagery. Int J Appl Earth Obs Geoinf 64:31–42

Mielcarek M, Stereńczak K, Khosravipour A (2018) Testing and evaluating different LiDAR-derived canopy height model generation methods for tree height estimation. Int J Appl Earth Obs Geoinf 71:132–143

Payero J, Neale C, Wright J (2004) Comparison of eleven vegetation indices for estimating plant height of alfalfa and grass. Appl Eng Agric 20:385

Qi J, Chehbouni A, Huete AR, Kerr YH, Sorooshian S (1994) A modified soil adjusted vegetation index. Remote Sens Environ 48:119–126

Rondeaux G, Steven M, Baret F (1996) Optimization of soil-adjusted vegetation indices. Remote Sens Environ 55:95–107

Rouse J, Haas R, Schell J, Deering D (1974) Monitoring Vegetation Systems in the Great Plains with ERTS Proceeding. In: Third earth reserves technology satellite symposium, Greenbelt: NASA SP-351

Schulze-Brüninghoff D, Hensgen F, Wachendorf M, Astor T (2019) Methods for LiDAR-based estimation of extensive grassland biomass. Comput Electron Agric 156:693–699

Stanton C, Starek MJ, Elliott N, Brewer M, Maeda MM, Chu T (2017) Unmanned aircraft system-derived crop height and normalized difference vegetation index metrics for sorghum yield and aphid stress assessment. J Appl Remote Sens 11:026035

Tucker CJ (1979) Red and photographic infrared linear combination for monitoring vefetation. Remote Sens Environ 8:127–150

Tunca E, Köksal ES, Çetin S, Ekiz NM, Balde H (2018) Yield and leaf area index estimations for sunflower plants using unmanned aerial vehicle images. Environ Monit Assess 190:1–12

van Iersel W, Straatsma M, Addink E, Middelkoop H (2018) Monitoring height and greenness of non-woody floodplain vegetation with UAV time series. ISPRS J Photogramm Remote Sens 141:112–123

Volpato L, Pinto F, González-Pérez L, Thompson IG, Borém A, Reynolds M, Gérard B, Molero G, Rodrigues FA Jr (2021) High throughput field phenotyping for plant height using UAV-based RGB imagery in wheat breeding lines: feasibility and validation. Front Plant Sci 12:185

Watanabe K, Guo W, Arai K, Takanashi H, Kajiya-Kanegae H, Kobayashi M, Yano K, Tokunaga T, Fujiwara T, Tsutsumi N (2017) High-throughput phenotyping of sorghum plant height using an unmanned aerial vehicle and its application to genomic prediction modeling. Front Plant Sci 8:421

Xie C, Yang C (2020) A review on plant high-throughput phenotyping traits using UAV-based sensors. Comput Electron Agric 178:105731

Xie T, Li J, Yang C, Jiang Z, Chen Y, Guo L, Zhang J (2021) Crop height estimation based on UAV images: methods, errors, and strategies. Comput Electron Agric 185:106155

Yuan W, Li J, Bhatta M, Shi Y, Baenziger PS, Ge Y (2018) Wheat height estimation using LiDAR in comparison to ultrasonic sensor and UAS. Sensors 18:3731

Yue J, Yang G, Li C, Li Z, Wang Y, Feng H, Xu B (2017) Estimation of winter wheat above-ground biomass using unmanned aerial vehicle-based snapshot hyperspectral sensor and crop height improved models. Remote Sens 9:708